ScienSage

Journal of Advanced Scientific Research

Available online through http://www.sciensage.info

ISSN
0976-9595
Research Article

IDENTIFICATION OF A POTENT AUTOPHAGY INHIBITOR IN LUNG AND BREAST CANCER

Priyanka Mudaliar[1], Apoorva Nalawade[1], Shine Devarajan, Jyotirmoi Aich*

School of Biotechnology and Bioinformatics, DY Patil Deemed to Be University, CBD Belapur, Navi Mumbai, Maharashtra, India

**Corresponding author:jyotirmoi.aich@dypatil.edu*

ABSTRACT

The incidence rate of both breast and lung cancer has escalated along with increased recurrence cases despite new treatment regimens. The inhibition of autophagy by particular medicines is a unique technique for broadening the range of treatment resistance in both of these cancers. The aim of the present investigation is to identify a potent autophagy inhibitor in lung and breast cancer. Different anti-malarial drugs were evaluated through *in silico* tools for their autophagy inhibiting potential in lung and breast cancer. Through a detailed text mining approach, a database of vital genes involved in autophagy in lung and breast cancer was curated. Molecular docking of these targets with different anti-malarial drugs was performed using AutoDock and AutoDock Vina. Mefloquine exhibited the best affinity towards all targets in lung cancer and hence it was chosen for further *in vitro* validation in A549 cells. Similarly, Artemisinin was selected for further *in vitro* evaluation in MCF-7 cells. When A549 cells were treated with varied concentrations of Mefloquine, significant cell death was observed with increased concentrations of drug and the IC_{50} of Mefloquine was determined to be 6.315 µM for 24 hrs. MCF-7 cells too showed cell death when treated with Artemisinin and the IC50 value obtained for the drug was found to be 1.138µM for 72 hrs. Based on these investigations, we can state conclusively that Mefloquine and Artemisinin appear to be potential autophagy inhibiting candidates for therapeutic treatment of lung and breast cancer respectively, in comparison to other known drugs.

Keywords: Autophagy Inhibitor, Lung Cancer, Breast Cancer, Drug Repurposing, Antimalarial Drugs, Molecular Docking.

1. INTRODUCTION

Cancer is quite possibly the most deadly and unwavering disease with a fundamentally high pace of mortality around the globe than other illnesses. Lung cancer is by a long shot the main source of cancer death in people, making up practically 25% of all deaths related to cancer. Lung cancer (2.21 million new cases) was the most frequent cancer in 2020 (in terms of new cases), and it was also the most prevalent cause of cancer death (1.80 million deaths) [1]. The adoption of targeted treatments and immunotherapies has resulted in survival benefits in a fraction of patients over the last two decades. Non-small cell lung cancer (NSCLC) and small cell lung cancer (SCLC) at all stages, on the other hand, had 5-year overall survival rates of 18.6% and 6%, respectively [2]. The most prevalent and active cancer in women is breast cancer. Survival rates of breast cancer have improved thanks to hormone treatment, chemical therapies, and radiotherapy. However, the incidence of breast cancer has continued to rise, most of the cases are of recurrence where the cancer has returned even after treatment [3]. As a result, developing novel therapeutic techniques is critical in order to enhance a patient's survival rates in both these cancers.

Expanding research has exhibited that autophagy inhibition might be a fitting remedial approach to treat cancer [4]. Autophagy is a cellular destruction system involving the elimination and debasing of inessential or malfunctioning organelles and proteins [5]. It is an evolutionarily conserved process that assists cells when responding to natural changes such as extreme circumstances like starvation and deprivation of nutrient. The components that are eliminated are first recycled and then orderly degraded in order to maintain homeostasis and viability for normal functioning and new cell formation [6]. It involves the double-membraned structures known as autophagosomes engulfing the cytoplasm along with its components and its fusion with

the lysosome leads to the release of the single-membrane autophagic body which is then degraded [5, 7]. During periods of metabolic cell stress, the cycle of autophagy is upscaled and expanded [8].

Many studies have reported autophagy as a double-edged sword in cancer- it can initiate and also suppress the growth of cancer cells [9-12]. Some research suggests that autophagy regulates numerous oncogenes and tumour suppressor genes while other research suggests that autophagy is involved in carcinogenesis, cancer growth, and cancer prevention [13]. Autophagy aids in the maintenance of metabolic needs under food shortage, genotoxic distress, growth factor depletion, and hypoxia [14]. However, depending on the stage of tumour growth, autophagy plays a contradictory function in carcinogenesis. It acts as a tumour suppressor by degrading possibly cancer-causing substances early in carcinogenesis. While, on the other hand, autophagy helps tumour cells survive at advanced stages by reducing stress in the microenvironment [10]. As a result, specifically targeting autophagy can be a therapeutic option for cancer treatment since inhibition of autophagy has been reported to improve the restorative adequacy in cancer therapy [4].

Autophagy involves several consecutive steps like sequestration, degradation, and amino acid/peptide generation which are mediated by the products of autophagic-related genes (ATGs) [15, 16]. Mechanisms like the mTOR (for nutrient), AMPK (for energy) and HIFs (for stress) regulate these ATG genes. These ATG genes, once activated, arrange and intervene the development of autophagosomes that convey intracellular components to the lysosome for degeneration [17]. So, targeting these genes using *in silico* methods addresses a novel methodology to expand the range of drug resistance in lung and breast cancers.

Antimalarial medicines are antiparasitic treatments that are used to cure malaria. These medicines have also been shown to have the ability to aid in the treatment of cancer [18]. The thought of such medications as conceivable anticancer medications depends on their capacity to meddle with significant oncogenic pathways, for example, Wnt-catenin/βSTAT3, and NF-kB alongside the arising part of mitochondria in interceding the anti-cancer impacts of antimalarials [19]. Among them, Chloroquine, Primaquine, and Mefloquine especially have been researched in the therapy of various sorts of cancers, both alone and in mix with chemotherapy [18, 20]. The toxicity of these medications is already recognised, so their usage in clinical trials can begin once their anti-cancer properties are well understood.

Molecular docking is a technique for studying the molecular behaviour of target proteins when they bind. It's a tool that is widely utilised in drug development. AutoDock, AutoDock Vina, and other docking applications are among the best.

We identified Artemisinin, Primaquine, Quinine, Chloroquine, Hydroxychloroquine, Mefloquine and Ferroquine based on their autophagy inhibiting potential through literature, taking into account the function of putative target receptors, such as certain autophagy related genes, in the initiation and progression of lung and breast cancer (Table 1 & 2). The purpose of our study was to represent the drug repurposing capability of these few antimalarial drugs and to identify a potent autophagy inhibitor from them in lung and breast cancer by various molecular docking approaches and *in vitro* studies. The *in silico* molecular docking analysis is based on the idea that antimalarials can interfere with the actions of the autophagy target receptors, causing their activity to be inhibited and cancer growth to be slowed.

Table 1:List of Genes involved with Autophagy in Lung Cancer

Gene In Lung Cancer	Activated In Autophagy	Inactivated In Autophagy	Upregulated In Autophagy	Downregulated In Autophagy	References
Beclin1				✓	[21]
LC3A				✓	[21]
ATG7	✓				[22]
ATG5	✓				[23]
DRAM2			✓		[24]
LAPTM4B				✓	[25]
ATG10			✓		[26]
TLR4		✓			[27]
Derlin-1		✓			[28]
p53	✓				[29]

These genes are either activated/inactivated/upregulated/downregulated in autophagy and may be responsible for tumour progression.

Table 2:List of Genes involved with Autophagy in Breast Cancer.

Gene In Breast Cancer	Activated in Autophagy	Reference
LC3	✓	[30]
ATG4A	✓	[31]
miRNA-638	✓	[32]
BIRC5	✓	[33]
TP63	✓	[33]
TRPM2	✓	[34]

These genes are either activated/inactivated/upregulated/ downregulated in autophagy and may be responsible for tumour progression

2. MATERIAL AND METHODS

2.1. Drugs and Reagents

Mefloquine and Artemisinin were obtained from a pharmacy. The cell lines (A549 and MCF-7) were procured from the National Centre for Cell Science (NCCS), Pune. Dulbecco's Modified Eagle's Medium (DMEM) and antibiotics [Penicillin-Streptomycin (10,000 Units/ml-10,000µg/ml)] were acquired from Cell Clone, Mumbai. Fetal Bovine Serum (FBS) and 0.25% Trypsin-EDTA were obtained from GIBCO. Other reagents used in the culture room were of analytical grade.

2.2. Cytotoxicity Assay

Cell based cytotoxicity assay was performed using A549 and MCF-7 cell lines. 5000 cells for A549 and 3500 cells for MCF7 were seeded in 200µl of complete medium in a 96-well plate and incubated in 5%CO_2 incubator at 37°C. Upon incubation for 24 & 72 hours, respectively, different concentrations of Mefloquine and Artemisinin (dissolved in DMSO) were added to the cells. Upon respective incubations of different drug in the cells, 5mg/ml of MTT solution was added to each well and incubated for 4hrs at 37°C. Formazon crystals was dissolved in DMSO and absorbance was read using a Biorad microplate reader at 570nm.

2.3. *In silico* Analysis

2.3.1. Software used for Molecular Docking

Molecular docking was performed between 7 autophagy inhibiting drugs and 10 autophagy genes in lung cancer (table 1) and 6 autophagy genes in breast cancer (table 2) to observe their binding and interaction. The docking was performed to narrow down the potent autophagy drug which can be further used for the target therapy in lung cancer and breast cancer. For performing the docking, AutoDock (version 1.5.6) and AutoDock Vina (version 1_1_2) were used for the study. Open Babel used for energy minimization and 3D conformer generation. The text editor software Perl IDE was also used along with Ubuntu software for giving commands required for docking. The BIOVIA Discovery Studio Visualizer (2019 version) for viewing the binding between ligand and receptor in 2D and 3D presentation was also used.

2.3.2. Screening for Receptors and Ligands

Literature search was done in PubMed and other similar databases to identify autophagy related genes that were upregulated or activated in lung cancer and breast cancer. After an extensive search, 10 genes (Table 1) were identified and narrowed down to be used as receptors for lung cancer and 6 genes (Table 2) were identified to be used as receptor for Breast cancer for docking. By reviewing numerous recorded literature findings, few FDA-approved antimalarial drugs were examined for their involvement in inhibiting autophagy in cancer. The 7 antimalarial drugs were selected as ligands by considering their autophagy inhibiting property for multi docking.

2.3.3. Structure Retrieval

The ligands were downloaded in .sdf format from PubChem database. The structures of the target proteins were retrieved from the RCSB Protein database in .pdb format.

2.3.4. Computational Analysis of the Antimalarial Drugs by Molecular Docking to Potential Target Proteins in Lung and Breast Cancer Cells

Discovery Studio Visualizer (DSV), Swiss PDB Viewer (SPDBV), AutoDock and AutoDock Vina were used to perform *in silico* analysis employing protein ligand binding approaches.

Ligands (drugs) were downloaded from PubChem in 3D conformer and the receptors of the respective genes were downloaded from Protein Data Bank in pdb format. DS Visualizer was used to remove undesired water molecules from the protein, as these molecules could interfere with the ligands in the docking process, resulting in inaccurate results. Energy minimization of the proteins was done using SPDBV. After energy minimization, the protein's minimised structure was checked for polar hydrogen based on atom types, steric clash avoidance, and hydrogen bond formation, and then

partial atomic charges, atomic solvation parameters, and fragmental volumes were assigned, and then further optimised using the AutoDock tool. During the molecular docking process, the default setup for receptor protonation (net charge 0) was used. Finally, using the same programme (AutoDock), the protein's pdb format was transformed to pdbqt format. A 3D grid was generated with the proper X-, Y-, and Z-coordinates for each receptor/target protein (Table 3) to analyse the favourable binding energy between the protein and the ligand, and the spacing value was set to 0.375 for the Grid Parameter File. After all this was done, multi-ligand docking was performed using AutoDock Vina which involved docking of a single receptor with all the ligands. This was done by using an established procedure which involved the energy minimization of the ligand files and their conversion to pdbqt file for the docking. This entire multi-ligand docking procedure was performed for all the receptors/target proteins.

Only the best docked molecules were further evaluated. The significant 2D and 3D interactions between the ligands and the receptors binding sites were obtained by importing the docking results into DS Visualizer.

Table 3:Grid Box Dimensions Listed for each Target Protein

Target Protein	X- Coordinate	Y- Coordinate	Z- Coordinate
Beclin1	0.443	0.440	0.637
LC3A	2.654	6.027	28.868
ATG7	31.423	-21.678	19.017
ATG5	13.514	12.374	-7.205
DRAM2	-13.831	--16.080	-14.896
LAPTM4B	-11.633	32.010	1.027
ATG10	-48.111	9.769	25.903
TLR4	-13.263	13.092	-15.779
Derlin-1	12.034	20.488	21.008
p53	-14.077	-0.221	23.579
LC3	4.251	-1.372	-2.785
ATG4A	80.284	72.042	67.811
miRNA-638	29.196	-16.270	49.495
BIRC5	-14.676	-10.768	-27.884
TP63	-4.491	3.482	55.197
TRPM2	46.777	28.622	41.428

2.4. Statistical Analysis

Microsoft Excel 2016 was used to conduct the statistical analysis. The data from the plate reader was first transferred here wherein the readings were corrected, percent inhibition, mean and standard deviation was calculated. These readings were then plotted on a bar graph to visualize the results for the drug. GraphPad 8.0, a computational regression analysis programme, was used to calculate the IC_{50} value of the drug.

3. RESULTS

This study involved *in silico* and *in vitro* studies of a few anti-malarial medications to see which among them best inhibited autophagy in lung and breast cancer cells. Different software for molecular docking was used in computational analyses. The lung cancer model A549 and breast cancer model MCF-7 was used for *in vitro* investigation which comprised of a cytotoxicity assay for the chosen drug.

3.1. Molecular Docking Results

Molecular Docking was performed for all of the seven ligands with each of the 10 receptors in lung cancer (table 1) and 6 receptors in breast cancer (table 2). Multi-ligand docking was carried out using AutoDock and AutoDock Vina. Table 4 and 5 show the drug binding scores in kcal/mol for all medications and autophagy targets in lung cancer and breast cancer, respectively.

3.1.1. Docking Analyses and Drug Interactions

Each of the autophagy target proteins in lung cancer examined in this study were BECN1, LC3A, ATG7, ATG5, DRAM2, LAPTM4B, ATG10, TLR4, Derl1, p53 and their 3D structures obtained from Protein Data Bank were 6HOI, 3WAN, 3H8V, 4ZW1, 5LVX, 4MYQ, 4NAW, 4G8A, 5GLF and 3V3B, respectively. For breast cancer, the selected autophagy target proteins were LC3, ATG4A, TRPM2, miRNA-638,

BIRC5, TP63 and their 3D structures obtained from Protein Data Bank were 3WAL, 2P82, 1QVJ, 3UEC, 6RU6, respectively.

The scoring function of AutoDock considers a pose as inputs and produces a number that indicates the probability that the pose reflects a favourable binding interaction. A low (negative) binding energy/afinity implies a stable system and, therefore, a potential binding interaction. Table 4 and 5 show the binding energies/affinities of all the best docked molecules in lung cancer and breast cancer, respectively. These docking results suggest that, in terms of estimated binding free energy, the best overall binding to most of the targeted proteins in lung cancer was demonstrated by Mefloquine and Artemisinin in breast cancer. Thus, only these best docked molecules were further evaluated. The analyses were carried out target by target utilising the BIOVIA Discovery Studio visualizer to check the ligand's effectiveness and the state of interaction, as detailed below.

Table 4:Binding Energy Results in Kcal/ mol between the target protein in lung cancer and all the ligands

BINDING ENERGIES (Kcal/mol) of all Receptor-Ligand Complexes										
RECEPTORS	**BECN1**	**LC3A**	**ATG7**	**ATG5**	**DRAM2**	**LAPTM4B**	**ATG10**	**TLR4**	**DERL1**	**P53**
LIGANDS										
Artemisinin	-7.4	-7.7	-7.1	-7.1	-8.3	-7.4	-8.3	-8.1	-7.9	-7.6
Primaquine	-6.1	-6.6	-5.7	-6.2	-6.5	-5.5	-6.6	-6.5	-6.2	-6.4
Quinine	-6.9	-7	-6.4	-6.3	-8.4	-6.9	-7.5	-7.3	-7	-7.1
Chloroquine	-6	-6.4	-5.6	6.9	-7	-7.9	-6.4	-7.3	-5.5	-5.7
Hydroxychloroquine	-6.2	-6.4	-5.9	-7.2	-7.7	-6.5	-6.5	-6.5	-5.7	-5.7
Mefloquine	**-8.1**	**-8**	**-7.4**	**-7.8**	**-9.1**	**-9.8**	**-8.4**	**-8.3**	**-8.5**	**-7.8**
Ferroquine	-6.6	-6.7	-5.6	-7.5	-8.3	-9	-7.3	-6.7	-7.2	-6

Table 5:Binding Energy Results in Kcal/ mol between the target protein in breast cancer and all the ligands

BINDING ENERGIES (Kcal/mol) of all Receptor-Ligand Complexes						
RECEPTORS	**LC3**	**TRPM2**	**ATG4A**	**miRNA-638**	**BIRC5**	**TP63**
LIGANDS						
Artemisinin	**-7.2**	**-8.6**	**-7.5**	**-7.6**	**-6.6**	**-6.1**
Chloroquine	-5.7	-7.1	-5.7	-6.9	-5	-4.2
Ferroquine	-6.8	-7.6	-6.2	-7.3	-5.8	-4.9
Hydroxychloroquine	-5.7	-7	-5.5	-6.2	-6.2	-4.4
Mefloquine	-7	-8.2	-6.9	-7.6	-6.5	-5.5
Primaquine	-6	-6.5	-5.5	-6.2	-5.7	-4.2
Quinine	-7	-8	-6.5	-7.1	-6	-6.1

3.1.2. Binding between Autophagy Target Proteins in Lung Cancer and Mefloquine

According to the docking results, Mefloquine binds at the active region of each protein, engaging with key residues with polar and non-polar interactions. The binding energy obtained for Mefloquine towards BECN1, LC3A, ATG7, ATG5, DRAM2, LAPTM4B, ATG10, TLR4, Derl1 and p53, was -8.1, -8, -7.4, -7.8, -9.1, -9.8, -8.4, -8.3, -8.5, and -7.8 kcal/mol, respectively, as shown in Table 4. Figures 1, 2, 3A and 3B depict the 3D and 2D positions of Mefloquine in the active site of each of the 10 autophagy targets in lung cancer. Table 6 lists all of the interacting amino acid residues in each Protein-Mefloquine complex, along with the types of bonds present.

3.1.3. Binding between Autophagy Target Proteins in Breast Cancer and Artemisinin

As per the docking results, Artemisinin binds to critical residues with polar and non-polar interactions in each protein's active region. The binding energy obtained for Artemisinin towards LC3, ATG4A, TRPM2, miRNA-638, BIRC5, TP63 was -7.2, -7.5, -8.6, -7.6, -6.6 and -6.1 kcal/mol, respectively, as shown in Table 5. The 3D and 2D positions of Artemisinin in the active site of each of the 6 autophagy targets in breast cancer are depicted in Figures 3C, 3D and 4. Table 7 provides all interacting amino acid residues in each protein-

Artemisinin complex, as well as the types of interactions that exist.

In the docking of Mefloquine with autophagy targets in lung cancer and Artemisinin with targets in breast cancer, conventional hydrogen bonds, halogen bonds, weak Van der Waals interactions, along with pi-alkyl and alkyl interactions were significant interactions that helped stabilise the ligand's conformation and intercalate the structure with the receptor's binding pocket.

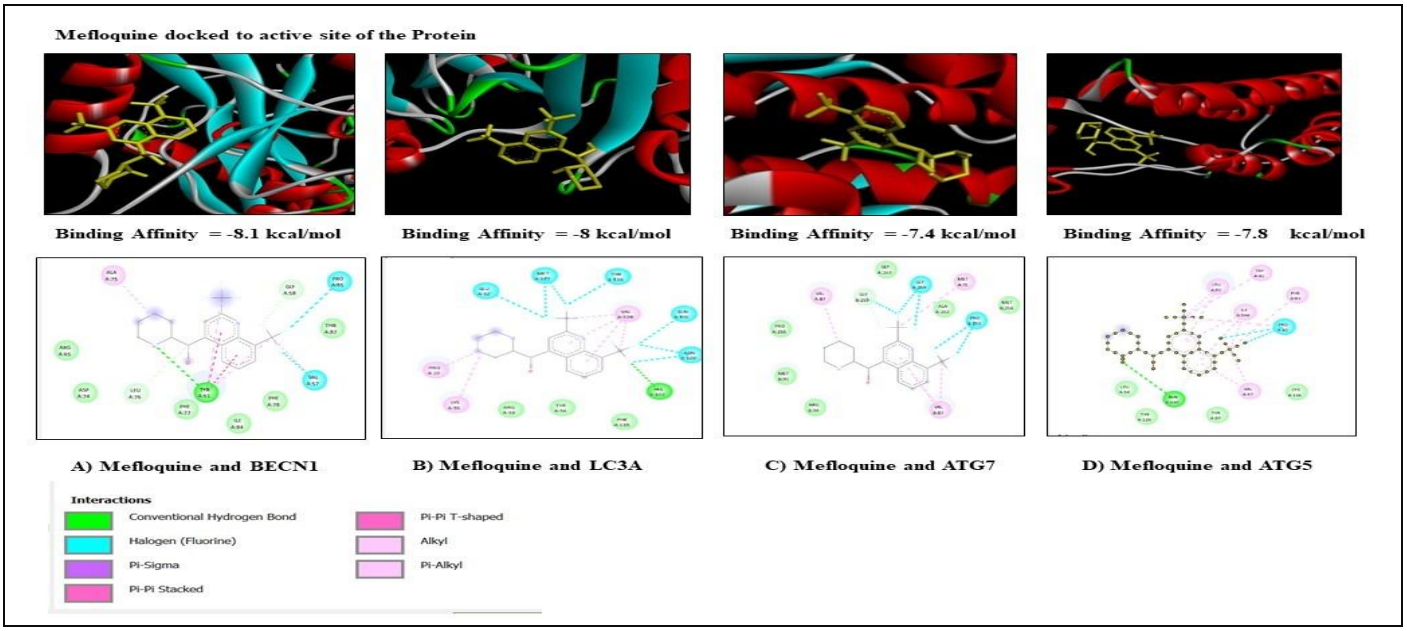

A- 3D binding pose interaction and 2D Ligplotof the interacting residues of BECN1 with Mefloquine B- 3D binding pose interaction and 2D Ligplotof the interacting residues of LC3A with Mefloquine C- 3D binding pose interaction and 2D Ligplotof the interacting residues ATG7 with Mefloquine D- 3D binding pose interaction and 2D Ligplotof the interacting residues of ATG5 with Mefloquine

Fig. 1:Docked poses of Mefloquine with the Target Proteins and the types of interactions

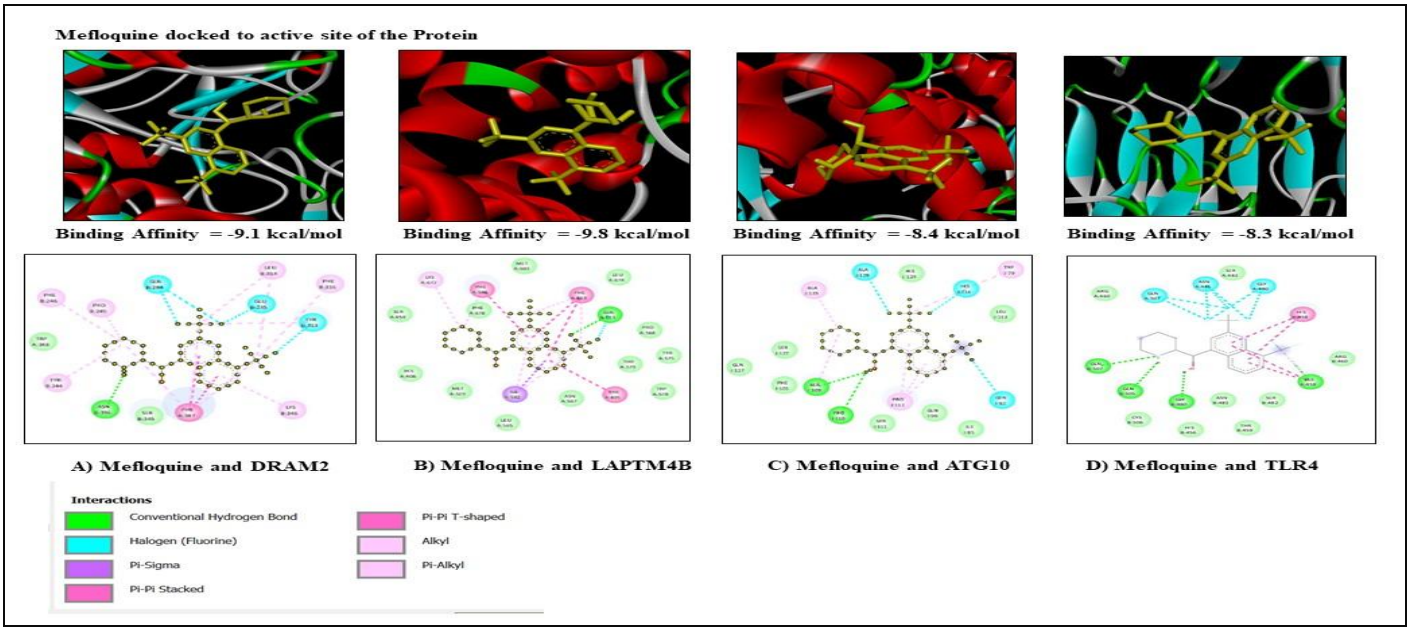

A- 3D binding pose interaction and 2D Ligplotof the interacting residues of DRAM2 with Mefloquine B- 3D binding pose interaction and 2D Ligplotof the interacting residues of LAPTM4B with Mefloquine C- 3D binding pose interaction and 2D Ligplotof the interacting residues ATG10 with Mefloquine D- 3D binding pose interaction and 2D Ligplotof the interacting residues of TLR4 with Mefloquine

Fig. 2:Docked poses of Mefloquine with the Target Proteins and the types of interactions

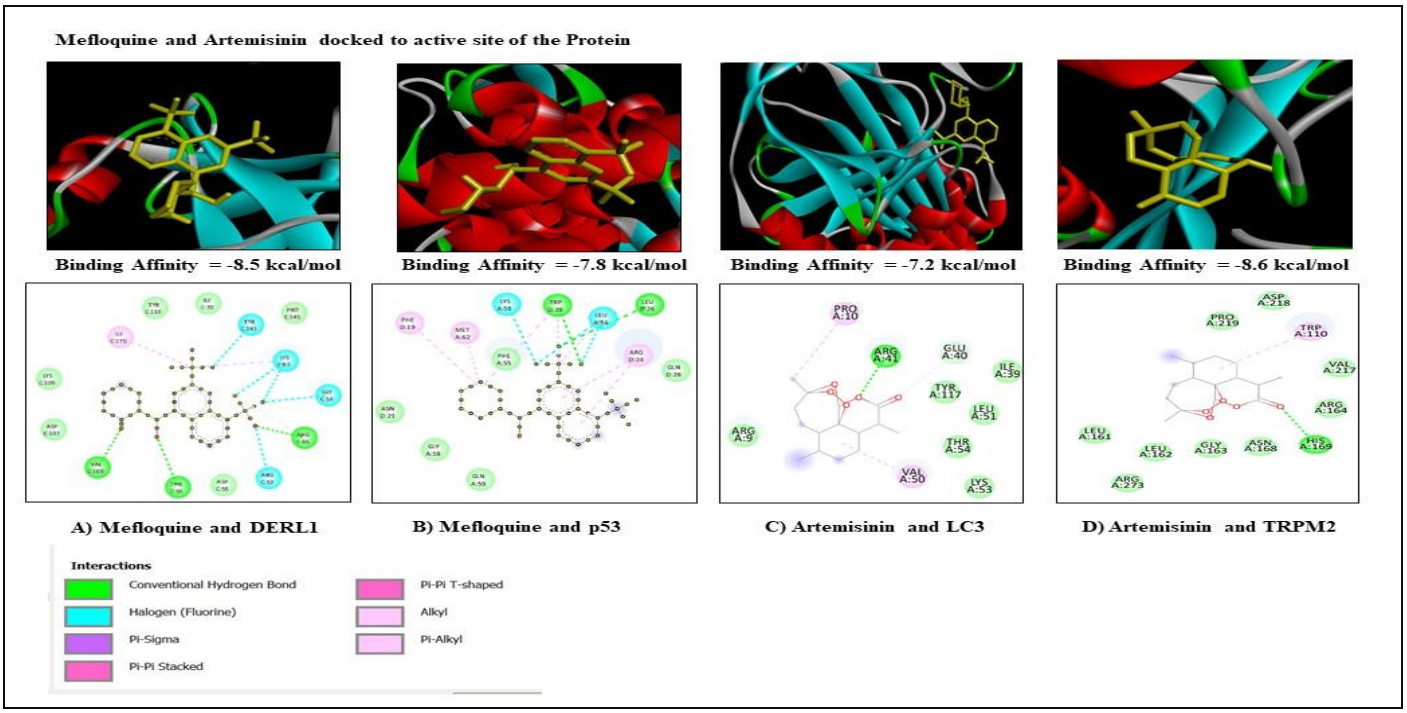

A- 3D binding pose interaction and 2D Ligplotof the interacting residues of DERL1 with Mefloquine B- 3D binding pose interaction and 2D Ligplotof the interacting residues of p53 with Mefloquine C- 3D binding pose interaction and 2D Ligplotof the interacting residues LC3 with Artemisinin D- 3D binding pose interaction and 2D Ligplotof the interacting residues of TRPM2 with Artemisinin

Fig. 3:Docked poses of Mefloquine and Artemisinin with the Target Proteins and the types of interactions

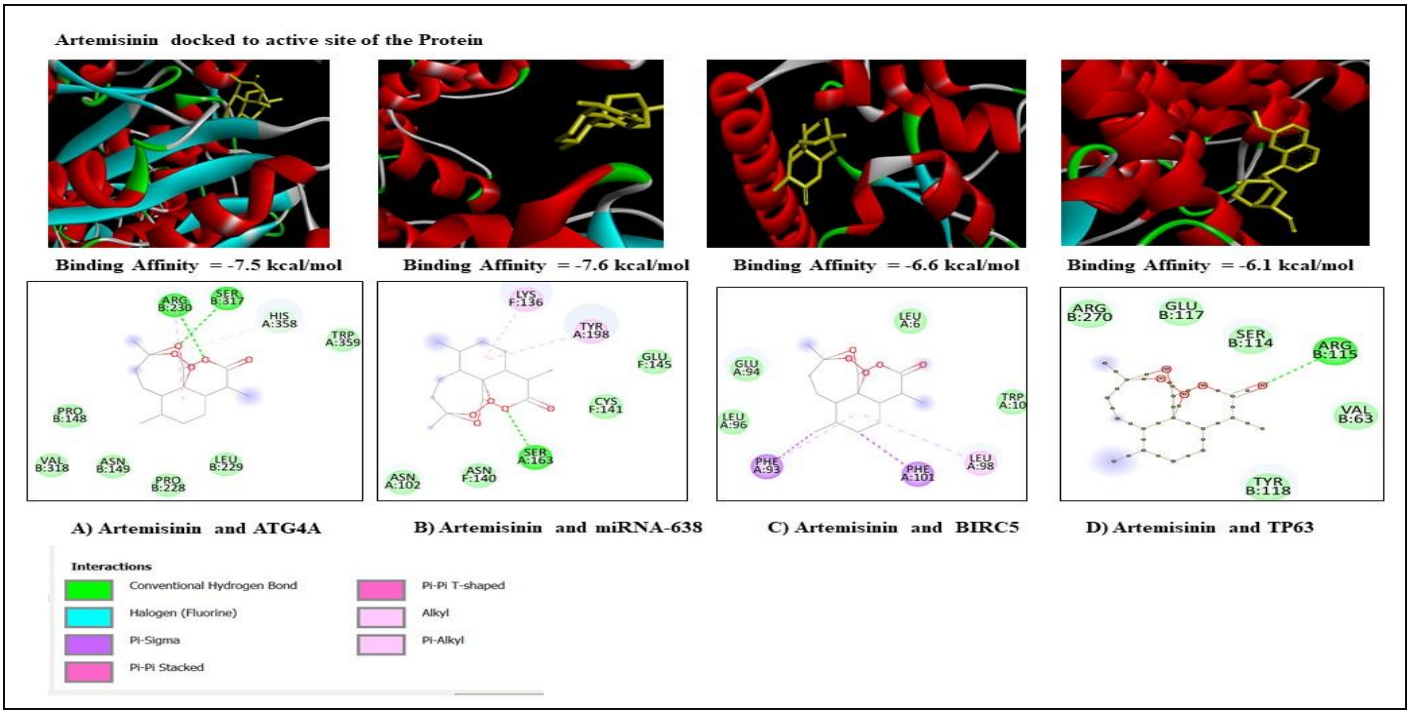

A- 3D binding pose interaction and 2D Ligplotof the interacting residues of ATG4A with Artemisinin B- 3D binding pose interaction and 2D Ligplotof the interacting residues of miRNA-638 with Artemisinin C- 3D binding pose interaction and 2D Ligplotof the interacting residues BIRC5 with Artemisinin D- 3D binding pose interaction and 2D Ligplotof the interacting residues of TP63 with Artemisinin

Fig. 4:Docked poses of Artemisinin with the Target Proteins and the types of interactions

Table 6: Types of molecular interactions and Amino acids involved in all the Targets and Mefloquine complex

TARGETS	BECN1	LC3A	ATG7	ATG5	DRAM2	LAPTM4B	ATG10	TLR4	DERL1	P53
MOLECULAR INTERACTION										
Van der Waals	ARG (A:65) ASP (A:74) PHE (A:77) ILE (A:84) PHE (A:78) THR (A:87)	ARG (A:53) TYR (A:54) PHE (A:135)	ARG(B:94) MET(B:91) PRO(A:255) GLY(A:263) ALA(A:262) MET(B:258)	LEU (A:94) TYR (A:139) TYR (A:94) CYS (A:136)	TRP (A:348) SER (B:345)	SER (A:454) PHE (A:678) MET (A:603) LEU (A:674) PRO (A:568) TYR (A:575) THR (A:579 TRP (A:578) ASN (A:567) LEU (A:565) MET (A:519) HIS (A:406)	HIS (J:124) LEU (J:113) ILE (I:85) GLN (I:99) SER (I:111) PHE (I:101) SER (J:127) GLN (I:137)	ARG (A:460) SER (A:482) ARG (B:460) SER (B:482) ASN (B:481)	LYS (C:109) TYR (C:110) ILE (C:70) PRO (C:145) ASP (C:55) ASP (C:107)	PHE (A:55) GLN (D:28) GLN (A:59) GLY (A:58) ASN (D:21)
Alkyl	ALA (A:75)	PRO (A:22) LYS (A:55) VAL (A:128)	VAL (A:87) MET (A:91)	LEU(A:92) ILE (A:146) VAL (A:87) PRO (A:82)	PRO (B:245) LEU (B:314)	ILE (A:582) LYS (A:677)	ALA (J:123) ALA (I:109) PRO (I:112)	HIS (B:458) HIS (A:458)	ILE (C:175) LYS (E:63)	LEU (A:54) MET (A:62) ARG (D:24)
Pi-Alkyl	TYR (A:61)	VAL (A:128)	VAL (B:87)	LEU (A:92) ILE (A:146) TRP (A:81) PHE (A:83) VAL (A:87)	PHE (B:246) PHE (B:316) LYS (B:346) PHE (A:347) TYR (B:244) TYR (B:313)	PHE (A:586) PHE (A:618)	TRP (J:79) PRO (I:112)	HIS (A:458)		TRP (D:23) PHE (D:19)
Hydrogen Bond	TYR (A:61)	HIS (A:102)		ASN (A:140)	ASN (B:396)	GLN (A:615)	ALA (I:109) PRO (I:110)	HIS (A:458) GLN (B:507) GLN (B:505) GLY (B:480)	ARG (E:65) THR (C:56) VAL (C:108)	TRP (D:23) LEU (D:26)
Halogen	PRO (A:85) VAL (A:57)	GLU (A:52) MET (A:127) TYR (A:126) GLN (A:101) ASN (A:100)	GLY (A:259) PRO (A:255)	PRO (A:82)	GLN (B:284) GLU (B:235) TYR (B:313)	GLN (A:615)	ALA (J:120) HIS (J:114) GLN (I:82)	GLN (A:507) ASN (A:481) GLY (A:480)	LYS (E:63) TYR (C:143) GLY (C:54) ARG (C:53)	LEU (A:54) LYS (A:51)
Pi-Donor Hydrogen Bond				ASN (A:140)						
Pi-Pi Stacked	TYR (A:61)				PHE (A:347)	PHE (A:618) PHE (A:586) TYR (A:405)				
Pi-Pi T shaped						PHE (A:618) PHE (A:586) TYR (A:405)				
Pi-Sigma						ILE (A:582)				

Table 7:Types of Molecular Interactions and Amino Acids involved in all the Targets & Artemisinin Complex

TARGETS	LC3	ATG4A	TRPM2	miRNA-638	BIRC5	TP63
MOLECULAR INTERACTION						
Van der Waals	ARG (A:9) LYS (A:53) LEU (A:51) THR (A:54) ILE (A:39) GLU (A:40)	PRO(B:148) VAL(B:318) ASN(B:149) PRO(B:228 LEU(B:229) HIS(A:358) TRP(A:359	PRO(A:219) ASP(A:218) VAL(A:217 ARG(A:164) ASN(A:168) GLY(A:163) LEU(A:162) LEU(A:161) ARG(A:273)	GLU(F:145) CYS(F:141) ASN(F:140) ASN(F:102)	LEU(A:6) TRP(A:10) GLU(A:94) LEU(A:96)	ARG(B:270) GLU(B:117) SER(B:114) VAL(B:63) TYR(B:118)
Hydrogen Bond	ARG (A:41)	ARG(B:230) SER(B:317)	HIS(A:169)	SER(A:163))		ARG(B:115)
Alkyl	ARG (A:50) PRO(A:10)			LYS(F:136) TYR(A:198)	LEU(A:98)	
Pi-Alkyl			TRP(A:110)	LYS(F:136) TYR(A:198)	LEU(A:98)	
Pi-Pi-Sigma					PHE (A:93) PHE (A:101)	

3.2. Cell Based Cytotoxicity Assay

The IC_{50} (Inhibitory Concentration-50) of a chemo-therapeutic drug is defined as the concentration of the agent that kills 50% of the cells in a particular sample. MTT is the most widely used approach for determining IC_{50} at the moment. In the proposed study, we performed MTT assay on A549 cells with Mefloquine and MCF-7 cells with Artemisinin.

3.2.1. In Vitro Studies in Lung Cancer Cell Line (A549)

Mefloquine is known to induce cell death via inhibiting autophagy in other cancers [20, 35, 36] To identify Mefloquine as a potent autophagy inhibitor in lung cancer, A549 cell line was the chosen lung cancer model for testing its effects *in vitro*. Cytotoxic assay was performed in which MTT was employed to measure cell death in A549 cells after they were exposed to the drug at various concentrations for 24 hours. The result of Mefloquine's effect on A549 cells is depicted in Fig. 5. The cells were treated with different concentrations of Mefloquine starting from 1 µM to 25 µM, for 24 hours and their respective absorbance was plotted using Microsoft Excel 2016. Dose response curve (Figure 6) was analysed by regression analysis in GraphPad Prism 8.0 and the IC_{50} was determined to be 6.315 µM. This suggests that 50% of A549 cells were killed by 6.315 µM of Mefloquine.

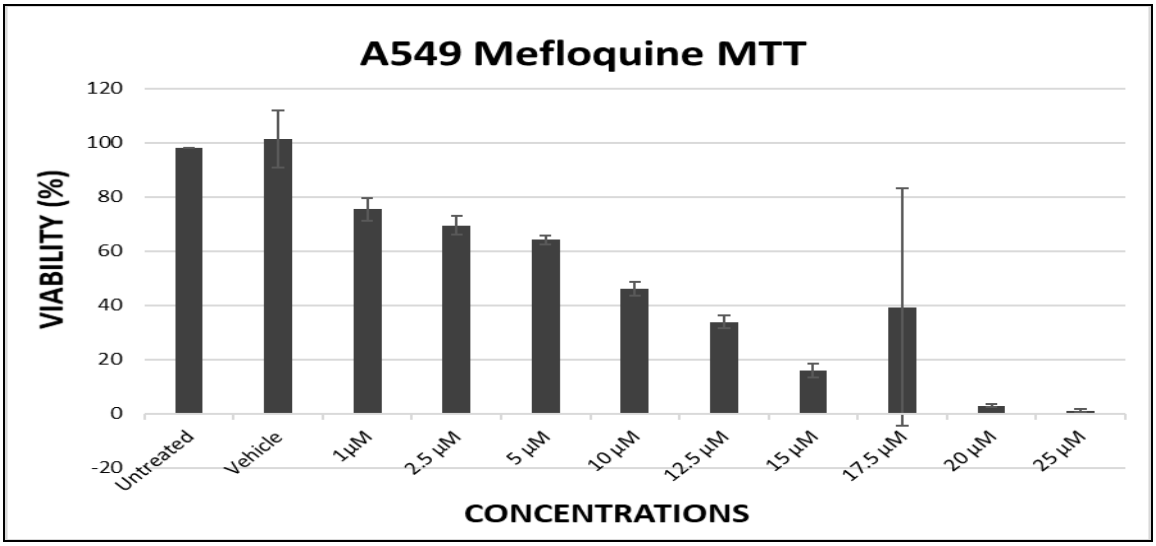

Fig. 5:Dose dependent cytotoxicity of Mefloquine in A549 cells using MTT assay

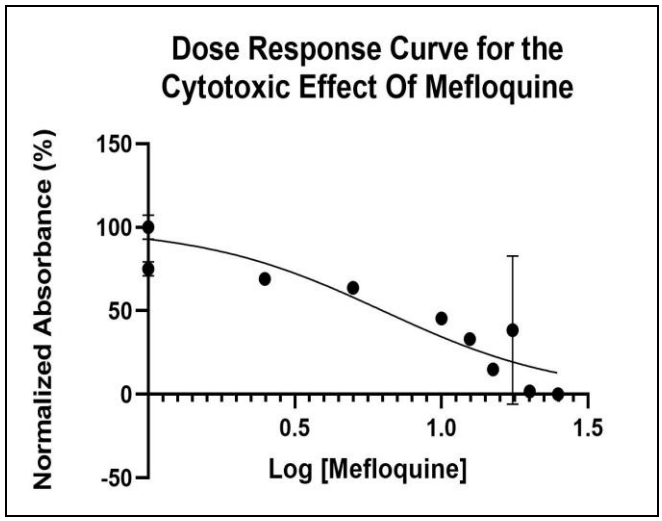

Fig. 6:Dose-response curve of IC_{50} value for Mefloquine on A549 cells

3.2.2. In Vitro Studies in Breast Cancer Cell Line (MCF-7)

Results obtained from molecular docking showed Artemisinin as the best docking drug with low energy. To analyse the efficacy of Artemisinin, cytotoxic assay was performed by using breast cancer cell line- MCF-7. The concentrations of Artemisinin used for the assay were 1µM, 2.5 µM, 5 µM, 10 µM, 12.5 µM, 15 µM, 17.5 µM, 20 µM and 25 µM. The graph in figure 7 depicts decrease in cell viability % as the concentration of Artemisinin dose increases. Values are expressed as mean ± SD. MCF-7 cells were treated with different concentrations of Artemisinin for 48 hr. At 20µm and 25µM the cell viability was observed to be less. And IC50 value for Artemisinin was found to be 1.138 µM. The IC50 value is the concentration at which a drug has half its maximum inhibitory effect. The IC50 value for

Artemisinin was found to be 1.138µM and was obtained from Graph Prism 7.0 (Fig. 8).

The graphical depictions in figs. 5- 8 indicate that when the concentration of Mefloquine in A549 cells and Artemisinin in MCF-7cells, was increased, the absorbance decreased at a constant pace, indicating that as the concentration of the drug increases, the cell density decreases. As a result, it may be inferred that A549 and MCF-7 cells had a strong response to Mefloquine's and Artemisinin's cytotoxic impact respectively. It is yet to be established if morphological changes occurred when both these cells were treated with the varying concentrations of both the drugs respectively.

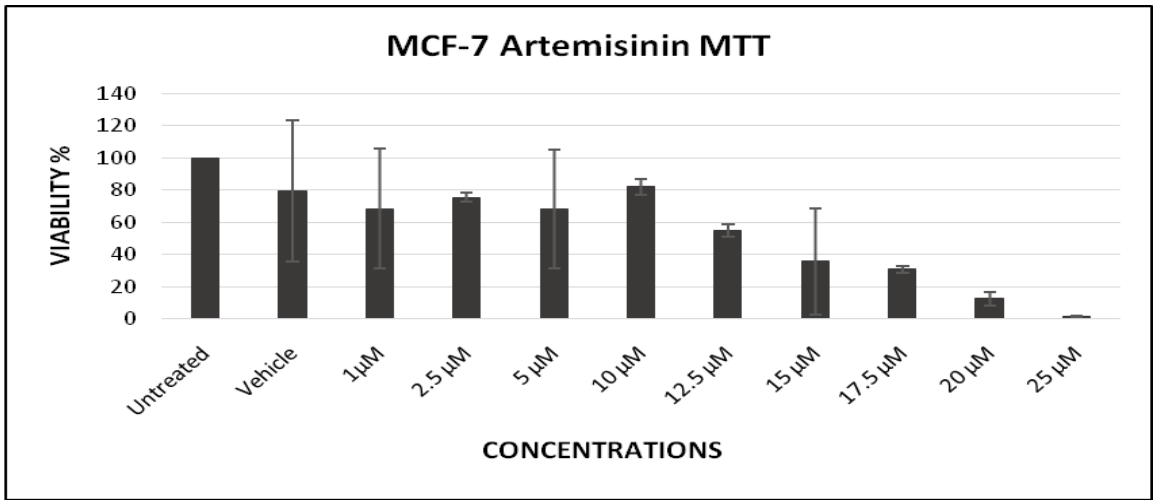

Fig. 7:Artemisinin induced cytotoxicity in Breast Cancer cells (MCF-7) evaluated using MTT assay

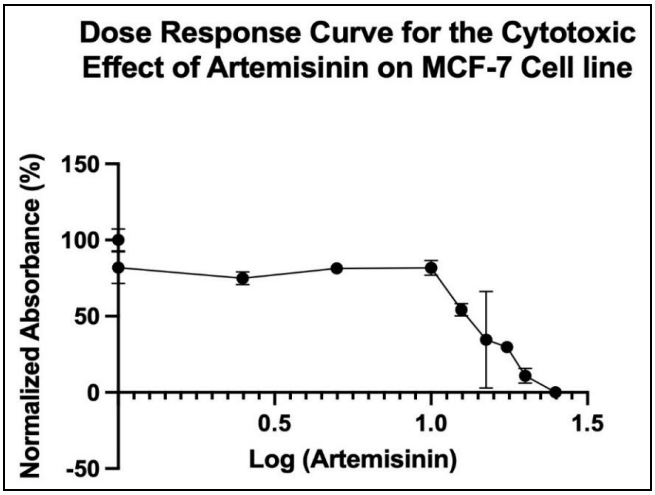

Fig. 8:Dose–response curve of IC_{50} value for Artemisinin on MCF-7 cells

4. DISCUSSION

In the previous decade, the field of oncology has seen significant changes in the manner with which cancer patients are overseen, with disserting the "one-size-fits-all" approach and expanding emphasis on precision medicine based on genomic variants. Clinical trials in oncology are presently being planned where patients are selected by the genetic profile of their tumours. Utilization of these new predictive and prognostic tools, alongside newly discovered repurposed drugs can help create a therapeutic treatment for cancer. The introduction of new therapies, such as targeted therapy and immune checkpoint inhibition, has changed the way patients with lung and breast cancer are treated and enhanced their therapeutic results substantially. However, tumour resistance to cytotoxic chemotherapy is a complex challenge in cancer therapy. Autophagy assumes an important part in keeping up cell homeostasis and genomic integrity by debasing matured or broken-down organelles and harmed or misfolded proteins. It is increased in response to metabolic and therapeutic stress and has been linked to cancer recurrence. By targeting ATGs in lung and breast cancer along with carrying on computational and laboratory investigations on them with already established drugs, we can find a novel and potent autophagy inhibitor that can be used in cancer treatment. Thus, in the present study, potential targets of autophagy in lung as well as breast cancer were scanned in literature and a list of genes was created. At the same time a list of potential autophagy inhibiting drugs was also sought out from the already established and approved inventory of drugs. Antimalarial drugs were analysed through *in silico*

molecular docking strategies with the targeted genes for their autophagy inhibiting capability. In computer-aided drug development, molecular docking was used to forecast which compounds will be most effective in binding to the target protein. The best drug binding sites towards the affinity of active site amino acids were tested using AutoDock and AutoDock Vina to predict the optimum drug binding sites.

In its docking with all of the autophagy target proteins in lung and breast cancer respectively, Mefloquine and Artemisinin displayed promising interactions with each protein's amino acids such as hydrogen bonds, non-covalent bonds and halogen bonds. These bonds helped stabilize the Drug-Protein complex by improving binding affinities. All of the halogen bonds of the Mefloquine and Protein complex involved Fluorine. Fluorine has been shown to have a significant impact on the hydrophobic interaction between the drug molecule and the receptor due to its potential to improve the lipophilicity of the molecule. As a result, it has a significant impact on the drug-receptor interaction, resulting in increased drug activity. Further, cell-based cytotoxicity assay of mefloquine and artemisinin in A549 and MCF-7 cells, respectively confirmed the anticancer property and hence, it can be inferred that both these drugs could be used as an autophagy inhibitor in lung and breast cancer therapy, respectively.

5. CONCLUSION

Antimalarial drugs were studied *in silico* and *in vitro* to see how effective they are at inhibiting autophagy in lung and breast cancer. The drugs were docked to potential target genes in lung and breast cancer cells for computational analysis using AutoDock and AutoDock Vina, and a comparative evaluation was performed. The findings of the docking studies suggested that all the drugs showed a stable interaction with the genes, however, Mefloquine stood the best among all in lung cancer and Artemisinin in breast cancer. Thus, on A549 and MCF-7 cells, a cytotoxic assay of Mefloquine and Artemisinin was performed respectively. The IC_{50} of Mefloquine was determined to be 6.315 μM during a 24 hours incubation period with the drug in lung cancer cells and the IC_{50} of Artemisinin was found to be 1.138μM during a 72 hours incubation period with the drug in breast cancer cells. Thus, the current work concludes that Mefloquine and Artemisinin may be regarded as powerful drugs for suppressing autophagy and thus can be utilised for targeted therapy in lung and breast cancer, respectively, based on *in silico* studies and in vitro validation. The drugs can be further examined individually or can also be combined with other therapeutic agents in order to delineate its role as an adjuvant in chemotherapy. Improvements in techniques can be made to obtain synergizing results even with multi-drug resistance cell lines. *In-vitro* and *in-vivo* research on different lung and breast cancer models can also be conducted to further study the medicines for the diagnosis and monitoring of both diseases.

6. ACKNOWLEDGEMENTS

Authors would like to acknowledge School of Biotechnology and Bioinformatics, DY Patil Deemed To Be University, Navi Mumbai for providing all the necessary facilities.

Disclosure statement

The authors declare no conflict of interest.

7. REFERENCES

1. Cancer.https://www.who.int/news-room/fact-sheets/detail/cancer, 2021.
2. Wang M *et al.*, *Int. J. Mol. Med*, 2020 ; **46(3)**:1816-1826 .
3. Macdonald S , Oncology R, and General M. *J. R. Soc. Med*, 2016; **70(8)** :515-517.
4. Liu T, Zhang J, Li K, Deng L, and Wang H. *Front. Pharmaco*, 2020; **11(1):**1-14.
5. Glick D, Barth S, and Macleod K F. *Journal of Pathology*, 2010; **221(1):**3-12.
6. Boya P, Reggiori F, and Codogno P. *Nature Cell Biology*, 2013; **15(7):**713-720.
7. Klionsky D J. *Curr. Biol*, 2005; **15(8):**282-283.
8. "What is Autophagy?" https://www.news-medical.net/life-sciences/What-is-Autophagy.aspx (accessed Mar. 25, 2021).
9. Nazio F, Bordi M, Cianfanelli V, Locatelli F, and Cecconi F. *Cell Death Differ*, 2019; **26(4):**690-702.
10. Chavez-Dominguez R, Perez-Medina M, Lopez-Gonzalez J S, Galicia M-Velasco, and Aguilar-Cazares D. *Front. Oncol*, 2020; **10(1):**1-19.
11. Liu G *et al., Int. J. Mol. Sci,* 2017**; 18(2):**1-17.
12. Yun C W and Lee S H. *Int. J. Mol. Sc.*, 2018; **19(11):**1-18.
13. Yu L, Chen Y, and Tooze SA. *Autophagy*, 2018; **14(2):**207-215.
14. Kroemer G, Mariño G, and Levine B. *Molecular Cell*, 2010**; 40(2):**280-293.
15. Sun K *et al.Cell Biosci*, 2013; **3(1):**1-8.
16. N. Mizushima, "Autophagy:Process and function,"

Genes Dev., vol. 21, no. 22, pp. 2861-2873, 2007, doi:10.1101/gad.1599207.
17. E. White, J. M. Mehnert, and C. S. Chan, "Autophagy, Metabolism, and Cancer," *Clin. Cancer Res.*, vol. 21, no. 22, pp. 5037-5046, 2015, doi:10.1158/1078-0432.CCR-15-0490.
18. CHOI A.R, KIM J.H, WOO Y.H, KIM H.S, and YOON.S. *Anticancer Res*, 2016; **36(4):**1-18.
19. Duarte D and Vale N. *Biomolecules*, 2020; **10(12):**1-20.
20. Sharma N *et al.Cancer Lett*, 2012; **326(2):**143-154.
21. PubMed.https://pubmed.ncbi.nlm.nih.gov/18184459/, 2021; 2021.
22. Guo J.Y *et al. Genes Dev*, 2013; **27(13):**1447-1461.
23. N. M *et al.J. Cell. Biochem*, 2018; **120(2):**1924-1931.
24. Wudu M *et al.J. Exp. Clin and Cancer Res*, 2019; **38(1):**20-28.
25. Maki Y *et al. Sci. Rep*, 2015; **5(1):**1-18.
26. Xie K *et al. Int. J. Cancer*, 2016; **139(7):**1564-1573.
27. Kim M.J *et al. Cancers (Basel)*, 2020; **12(11):**1-20.
28. Xu L *et al. Cancer Cell Int*, 2014; **14(1)**.
29. Saini H, Hakeem I, Mukherjee S, Chowdhury S, and Chowdhury R. *J. Oncol,* 2019; 2019.
30. Verma A.K *et al.* 2021; 2021.
31. Du J. X *et al.Gene*, 2020; **762:**144974.
32. Ren Y, Chen Y, Liang X, Lu Y, Pan W, and Yang M. *Cancer Lett*, 2017; **390:**126-136.
33. Han. B *et al.Aging (Albany NY)*, 2020; **12(13):**13318.
34. Miller B.A. *Cell Calcium*, 2019; **80:**8-17.
35. Mereddy G.R and Ronayne C.T. *Transl. Med*, 2018; **08(01):**8-11.
36. Kim J.H, Choi A.R, Kim Y.K, and Yoon S. *Biochem. Biophys. Res. Commun*, 2013; **441(3):**655-660.